Arctic sea ice response to atmospheric forcings with varying levels of anthropogenic warming and climate variability

Jinlun Zhang,[1] Michael Steele,[1] and Axel Schweiger[1]

Received 4 August 2010; revised 8 September 2010; accepted 20 September 2010; published 28 October 2010.

[1] Numerical experiments are conducted to project arctic sea ice responses to varying levels of future anthropogenic warming and climate variability over 2010–2050. A summer ice-free Arctic Ocean is likely by the mid-2040s if arctic surface air temperature (SAT) increases 4°C by 2050 and climate variability is similar to the past relatively warm two decades. If such a SAT increase is reduced by one-half or if a future Arctic experiences a range of SAT fluctuation similar to the past five decades, a summer ice-free Arctic Ocean would be unlikely before 2050. If SAT increases 4°C by 2050, summer ice volume decreases to very low levels (10–37% of the 1978–2009 summer mean) as early as 2025 and remains low in the following years, while summer ice extent continues to fluctuate annually. Summer ice volume may be more sensitive to warming while summer ice extent more sensitive to climate variability. The rate of annual mean ice volume decrease relaxes approaching 2050. This is because, while increasing SAT increases summer ice melt, a thinner ice cover increases winter ice growth. A thinner ice cover also results in a reduced ice export, which helps to further slow ice volume loss. Because of enhanced winter ice growth, arctic winter ice extent remains nearly stable and therefore appears to be a less sensitive climate indicator. **Citation:** Zhang, J., M. Steele, and A. Schweiger (2010), Arctic sea ice response to atmospheric forcings with varying levels of anthropogenic warming and climate variability, *Geophys. Res. Lett.*, *37*, L20505, doi:10.1029/2010GL044988.

1. Introduction

[2] Will the Arctic Ocean become ice-free during summer under continued anthropogenic warming (AW), and if so, when? This question captures public interest in climate change and presents a challenge for science. Global coupled climate models (GCMs) are useful tools for projecting future sea ice response to AW. However, a majority of GCMs used for the Intergovernmental Panel on Climate Change Fourth Assessment Report (IPCC AR4) underestimate the sensitivity of sea ice to AW in the past by underestimating the observed decline of sea ice extent [*Stroeve et al.*, 2007]. Further, GCMs, though steadily improving, are often unable to capture the observed magnitudes and spatial patterns of sea ice thickness, leading to a wide range in future projections [*Intergovernmental Panel on Climate Change* (*IPCC*), 2007; *Holland et al.*, 2010]. This problem has been addressed by adjusting model projections using observed ice extent [e.g., *Wang and Overland*, 2009]. Another approach is to extrapolate observed trends using model results [*Maslowski*, 2010]. However, the resulting broad range of projections about when the Arctic Ocean will be ice-free in summer, from ~2016 to near the end of the 21st century, highlights the challenge in projecting future sea ice responses to AW.

[3] This study explores arctic sea ice responses to future AW in a model that captures the observed spatiotemporal variability of sea ice in the past. We present an interim approach that aims to examine future response from an angle that avoids some of the difficulties associated with the sea ice projections from the AR4 generation of GCMs. The approach is based on an arctic ice–ocean model, the Pan-arctic Ice–Ocean Modeling and Assimilation System (PIOMAS), which has been shown to reproduce the observed variability both in spatial patterns and in trends of ice concentration, extent, and thickness [*Zhang et al.*, 2008]. PIOMAS is used here for a series of numerical experiments over 2010–2050 driven by forcing fields generated by projecting GCM estimated increases in arctic SAT onto historical atmospheric forcing fields. A similar approach was used by *Sou and Flato* [2009] to project future sea ice loss in the Canadian Archipelago region. Use of an uncoupled ice–ocean model of course does not allow feedbacks with the atmosphere. The underlying assumption in this approach is that the effects of those feedbacks are represented by the GCM estimated SAT changes imposed in the atmospheric forcing fields. Support for this assumption comes from an examination of an ensemble of GCMs that show high correlations (>0.96) between changes in sea ice extent and changes in SAT [*Ridley et al.*, 2007], suggesting that the combined effects of feedbacks on sea ice are well represented in the temperature response of the GCMs.

2. Model, Forcings, and Numerical Experiments

[4] The numerical experiments consist of a hindcast (HC) over 1978–2009 and four future projections over 2010–2050. The HC is driven by daily NCEP/NCAR reanalysis forcing data including surface winds, SAT, specific humidity, cloudiness, precipitation, and evaporation [*Zhang et al.*, 2008]. SAT and cloudiness are used to calculate surface downward shortwave (DSWR) and longwave (DLWR) radiation forcing following *Parkinson and Washington* [1979]. River runoff climatology is from *Hibler and Bryan* [1987]. No assimilation is performed.

[5] The future projections are driven by atmospheric forcings created by projecting GCM estimated arctic SAT increases onto the historical NCEP/NCAR reanalysis forcing in a way somewhat similar to *Sou and Flato* [2009]. Under the AW scenarios of increased emissions of greenhouse gases, IPCC GCMs projected that arctic SAT on average would increase ~2–4°C by 2050 [*IPCC*, 2007]. Based on

[1]Polar Science Center, Applied Physics Laboratory, University of Washington, Seattle, Washington, USA.

0094-8276/10/2010GL044988

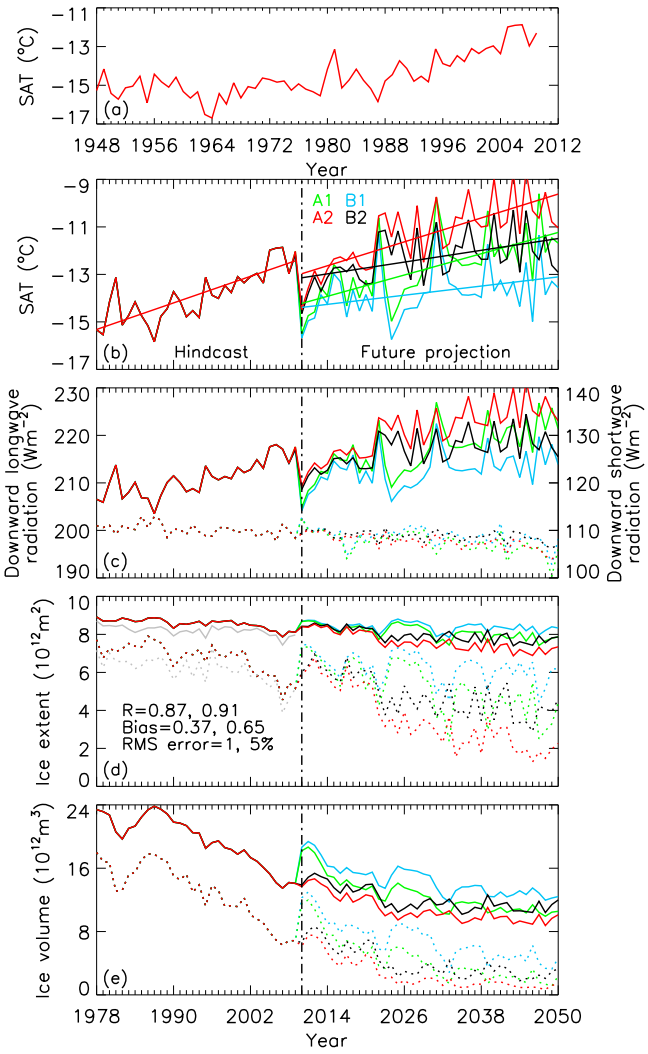

Figure 1. (a) Annual mean NCEP/NCAR reanalysis surface air temperature (SAT) over the Arctic Ocean, (b) annual mean reanalysis SAT over 1978–2009 used for the hindcast and constructed SATs over 2010–2050 for the four (A1, A2, B1, B2) future projections, (c) annual mean downward longwave radiation (solid line) and downward shortwave radiation (dash line), (d) simulated and satellite observed (gray line) annual (solid) and September (dotted) mean ice extent, and (e) simulated annual (solid) and September (dotted) mean ice volume. Model–data correlation (R) and model bias and root-mean-square (RMS) error for annual and September means are indicated in Figure 1d. Satellite ice concentration data are acquired from National Snow and Ice Date Center. The vertical dot-dash line marks the year 2010 when future projections start.

such projections, two scenarios are considered to approximate varying levels of AW in the atmospheric forcings: AW1 with an average SAT increase of 4°C by 2050 and AW2 with an increase of 2°C. Because of the inherent historical climate variability (CV) in the historical forcing, how the historical forcing is specified affects the CV in the future forcings. To examine sea ice response to varying future CV, two levels of historical CV are incorporated into the future forcings through two forcing pools from which the NCEP/NCAR reanalysis data for the past years are randomly picked one year at a time for the future years (2010–2050). One pool is over 1948–2009 and the other 1989–2009. Due to the positive SAT trend over 1948–2009, which includes both natural and anthropogenic changes, the 1948–2009 pool has a greater SAT range than the 1989–2009 pool and thus provides a greater level of historical CV. To create the atmospheric forcings for 2010–2050 under these two levels of AW and CV, the NCEP/NCAR reanalysis SAT is first randomly picked from either of the two pools and then either of the two SAT increases is superposed on the picked SAT linearly in time such that $SAT_i^k = SAT_j^k + \Delta SAT \times (i - 2009)/(2050–2009)$, where i = 2010,…. 2050, j is a randomly picked year from either the 1948–2009 or the 1989–2009 pool, k represents each model grid cell, and ΔSAT = 2°C, 4°C. Here for simplicity, constant values of ΔSAT are used. However, an ad hoc air–ice interaction is implemented in the model such that SAT ≤0 if the simulated ice concentration is above 50%.

[6] The IPCC GCMs also project increases in precipitation, evaporation, river runoff, and cloudiness (denoted collectively as PERC) in the Arctic. In particular, the projected increase in the annual mean precipitation, based on the A1B scenario, varies from ~5 to 14% by 2050, with an ensemble median of ~9% [*IPCC*, 2007]. To further simplify the forcings, the rates of increase in annual mean PERC are all fixed at 8% for AW1 and 4% for AW2 and are superposed also linearly in time on the corresponding NCEP/NCAR reanalysis data or the river runoff of *Hibler and Bryan* [1987] such that $PERC_i^k = PERC_j^k \times [1 + \Delta PERC \times (i - 2009)/(2050–2009)/100]$, where $\Delta PERC$ = 4%, 8%.

[7] It must be stressed that a series of simplifications are made to create the future forcings. For example, while allowing interannual variability, the random selection of historical forcing one year at a time removes decadal variability. No modifications are made to the selected historical surface winds, which does not reflect the possible changes in cyclone behavior and atmospheric circulation in a warmer Arctic [*Simmonds and Keay*, 2009]. Furthermore, feedbacks between changes in the ice–ocean system and atmospheric temperature, humidity, and clouds are not directly represented in the numerical experiments without an atmospheric model component. However, the effects of these feedbacks are assumed to be approximately represented by the prescribed increases in SAT and PERC and the corresponding changes in surface radiation. The two levels of future AW and historical CV adopted here are considered to be reflective of the uncertainties in climate sensitivity of IPCC AR4 models.

[8] Combinations of two AW scenarios and two pools of historical forcing comprise four future projection experiments. Case A1 (A2): ΔSAT = 4°C and $\Delta PERC$ = 8% are superimposed on the NCEP/NCAR reanalysis forcing randomly picked one year at a time from the 1948–2009 (1989–2009) pool. Case B1 (B2): ΔSAT = 2°C and $\Delta PERC$ = 4% are superposed on the reanalysis forcing randomly picked from the 1948–2009 (1989–2009) pool.

3. Behavior of Future Forcings

[9] The NCEP/NCAR reanalysis SAT shows warm years during 1989–2009 and some cold years pre-1989 (Figure 1a). There is a SAT increase of ~3°C from 1978 to 2009 with considerable interannual fluctuation (Figure 1b), suggesting significant historical CV. Starting with a SAT drop in 2010,

Table 1. Linear Trends in Annual Mean SAT, Observed and Simulated September Ice Extent, and Simulated September Ice Volume Over 1978–2009 (HC) and 2010–2050 (B1, B2, A1, and A2)[a]

Case	Annual Mean SAT (°C yr^{-1})	Observed Ice Extent (10^{12} m^2 yr^{-1})	Simulated Ice Extent (10^{12} m^2 yr^{-1})	Simulated Ice Volume (10^{12} m^3 yr^{-1})	Mean Ice Extent (10^{12} m^2)	Mean Ice Volume (10^{12} m^3)
HC	0.093	−0.055	−0.066	−0.34	6.8 (100)	13.0 (100)
B1	0.032		−0.028	−0.18	5.5 (81)	3.8 (29)
B2	0.041		−0.066	−0.13	4.2 (62)	2.7 (21)
A1	0.075		−0.084	−0.21	3.3 (49)	1.6 (12)
A2	0.084		−0.118	−0.14	1.9 (28)	1.0 (8)

[a]Simulated 1978–2009 (HC) and 2047–2050 (four cases) mean September ice extent (10^{12} m^2) and ice volume (10^{12} m^3); in parentheses are corresponding values in percentage of the 1978–2009 mean September ice extent and volume.

because the randomly picked years from the two pools are all colder than 2009, the future SATs show different increasing trends over 2010–2050 with significant interannual fluctuations, as expected (Table 1 and Figure 1b). The increasing SAT trends of A1 and A2 are comparable to the reanalysis data over 1978–2009, while the increasing SAT trends of B1 and B2 are significantly less. Although A1 and A2 are created with the same ΔSAT = 4°C, the SAT magnitude and trend of A2 are greater than those of A1 (Table 1 and Figure 1b) because A2 consists of recent warm years picked from the 1989–2009 pool, whereas A1 consists of years picked from the 1948–2009 pool with a wider SAT range. An analogous relationship exists between B1 and B2.

[10] Increasing SAT and cloudiness over 2010–2050 lead to increasing DLWR (Figure 1c) calculated following *Parkinson and Washington* [1979]. There are slight decreases in DSWR because of increasing cloudiness (Figure 1c). However, the decreases in DSWR are much smaller than the increases in DLWR. Thus the varying levels of atmospheric warming with the four cases are represented by increases in both SAT and DLWR.

4. Results

[11] To validate PIOMAS as a suitable tool to study future sea ice responses, we examined its response to the past atmospheric forcing. Compared to satellite observations, the model overestimates ice extent of the Arctic Ocean defined as the Arctic Basin and the Barents Sea (Figure 1d). Mean model bias for September ice extent is 0.65×10^{12} m^2. Nevertheless, the simulated annual and September mean ice extents are highly correlated with the corresponding satellite observations over 1978–2009 (R = 0.87 and 0.91, respectively), with low RMS (root-mean-square) errors of 1 and 5%. The model captures winter ice edge locations for recent years (Figures 2a–2d). It underestimates (overestimates) summer ice extent in the Atlantic (Pacific) sector of the Arctic Ocean for 2006 (2008), while it estimates well the summer ice extents of 2007 and 2009 (Figures 2m–2p).

[12] The projected September ice extents for the four cases generally decrease over 2010–2050, but the rates depend on the levels of AW and CV (Figure 1d and Table 1). For example, the linear decreasing trend of B1 over 2010–2050 is significantly less than that of the HC over 1978–2009 (Table 1), indicating that a moderate future AW (ΔSAT = 2°C by 2050) combined with the reoccurrence of some of the colder years as in 1948–2009 would not reduce summer ice extent substantially by 2050 (Figures 2q and 2u). In contrast, the linear decreasing trend of A2 is much greater than that of the HC (Table 1), indicating that a higher AW (ΔSAT = 4°C by 2050) combined with the reoccurrence of recent warm years (1989–2009) would significantly reduce summer ice extent (Figures 2t and 2x), with a reduction of 4.9×10^{12} m^2 (72%) from the HC (1978–2009) mean of 6.8×10^{12} m^2 by 2050 (Table 1).

[13] Comparisons between A1 and B1 and between A2 and B2 suggest that if AW doubles from 2°C to 4°C by 2050, September ice extent would decrease an additional ~2.2×10^{12} m^2 (~32%) by 2050 from the 1978–2009 mean (Table 1). The September ice extent of A2 decreases the most; however, it is generally above 3.0×10^{12} m^2 before 2025 and, given the model's bias in overestimating ice extent during 1978–2009 (Figure 1d), is considered to be close to 1×10^{12} m^2 during 2044–2050 (Figure 1d and Table 1). This suggests that even with A2, the Arctic Ocean would not be ice free in summer (ice extent $\leq$~1×10^{12} m^2 [*Wang and Overland*, 2009]) until near 2050 (Figure 2x). Furthermore, because the September ice extent of A1 is generally above 3.0×10^{12} m^2 over the whole 2010–2050 period, there is a likelihood that, with ΔSAT = 4°C, the Arctic Ocean would not be ice free by summer 2050 (Figure 2w).

[14] The projected September ice extents are subject to interannual fluctuations in association with the historical CV incorporated in the atmospheric forcings (Figures 1d and 2). The fluctuations remain significant approaching 2050. Thus, even if the projected September ice coverage falls to a particularly low level or below 1×10^{12} m^2 in a certain year before 2050, it is likely to rebound substantially in later years. This suggests that it is difficult to pinpoint a particular year before 2050 from which the Arctic Ocean would be and remain ice free in summer.

[15] The projected September ice volumes decrease faster than the projected September ice extents (Figure 1e). The loss of September ice volume compared with the 1978–2009 September mean ranges from 71% with B1 to 92% with A2 by 2050 (Table 1). In contrast, the loss of September ice extent compared with the 1978–2009 September mean ranges from merely 19% with B1 to 72% with A2 (Table 1). The September ice volumes of A2 and B2 drop to very low levels as early as around 2025 and remain almost flat in the following years when the projected September ice extents continue to fluctuate significantly annually (Figures 1d and 1e). This suggests that summer ice volume is more sensitive to AW than summer ice extent while the latter is more sensitive to CV.

[16] The projected annual mean ice extents do not decrease substantially (Figure 1d). The decrease in annual mean ice extent for all four cases is less than 2.0×10^{12} m^2 over 2010–2050. Most of the decrease occurs in summer (Figures 1d and 2). In winter, the projected ice extents rarely

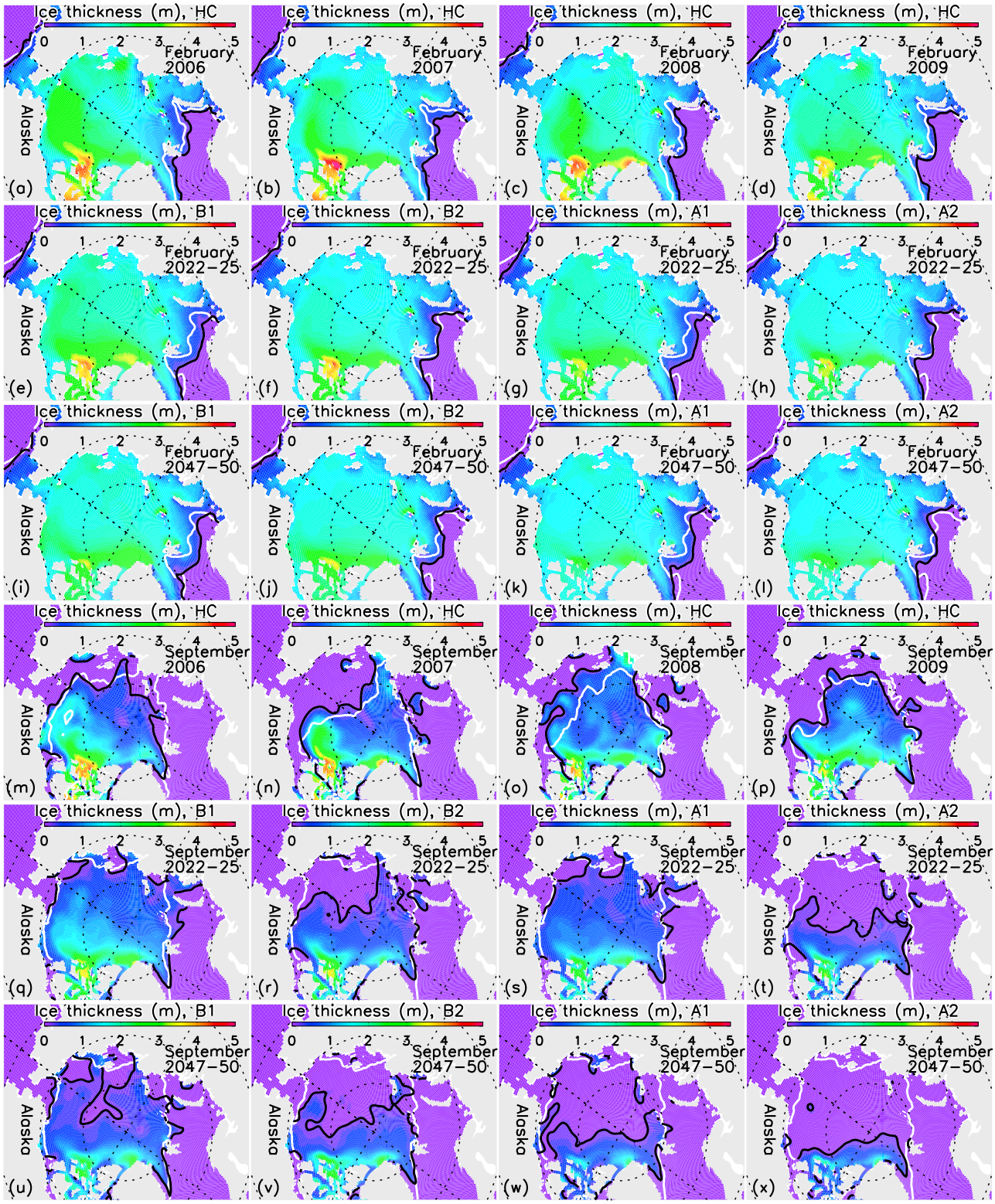

Figure 2. Hindcast (HC) of (a–d) February and (m–p) September mean ice thickness for 2006–2009 and future projections of (e–h) February 2022–2025, (i–l) February 2047–2050, (q–r) September 2022–2025, and (u–x) September 2047–2050 mean ice thickness for the four cases; black line represents corresponding simulated ice edge defined as 0.15 ice concentration. White line represents satellite observed February and September ice edge (Figures 2a–2d and 2m–2p) and 1978–2009 mean February and September ice edge (Figures2e–2l and 2q–2x).

Table 2. Linear Trends in Annual Mean Ice Volumes, Ice Export, Thermodynamic Ice Growth, Ice Melt, and Net Ice Change Over Periods of 1978–2009 (HC) and 2010–2025, 2035–2050, and 2010–2050 (B1, B2, A1, and A2)

Case	Ice Volume 78–09 (10^{12} m^3 yr^{-1})	Ice Volume 10–25 (10^{12} m^3 yr^{-1})	Ice Volume 35–50 (10^{12} m^3 yr^{-1})	Ice Volume 10–50 (10^{12} m^3 yr^{-1})	Ice Export 10–50 (10^{12} m^3 yr^{-2})	Thermodynamic Ice Growth 10–50 (10^{12} m^3 yr^{-2})	Ice Melt 10–50 (10^{12} m^3 yr^{-2})	Net Ice Change 10–50 (i = f − g − e)
HC	−0.30				−0.016	0.23	0.26	−0.012
B1		−0.29	−0.08	−0.14	−0.013	0.19	0.22	−0.014
B2		−0.25	−0.03	−0.09	−0.015	0.16	0.17	−0.000
A1		−0.38	−0.08	−0.17	−0.018	0.22	0.26	−0.017
A2		−0.30	−0.00	−0.11	−0.020	0.15	0.17	−0.001

deviate significantly from the 1978–2009 mean (Figures 2e–2l). Thus, winter ice extent is insensitive to AW before 2050.

[17] The projected annual mean ice volumes decrease substantially during 2010–2025, with the linear decreasing trends comparable to the HC trend over 1978–2009 (Figure 1e and Table 2). They decrease at lower rates in later years, particularly over 2030–2050 (Table 2) even as SAT continues to increase. One reason is that, although ice melt mainly in summer continues to increase with increasing SAT (Figure 3c), thermodynamic ice growth mainly in winter increases too (Figure 3b) because thinner ice has a higher growth rate [*Bitz and Roe*, 2004]. In fact, the linear increasing trends of annual mean ice growth over 2010–2050, like those of annual mean ice melt, are comparable to the trends over 1978–2009 (Table 2). Another reason is that ice export from the Arctic decreases in the future, just as in 1978–2009 (Figure 3a and Table 2), because of reduced ice thickness (Figure 2) [*Holland et al.*, 2010]. As a result, the linear decreasing trends of the net ice change (ice growth minus ice melt and ice export) in the Arctic are small, especially with A2 and B2 (Table 2), leading to much lower trends in decreasing ice volume during particularly 2030–2050 (Table 2).

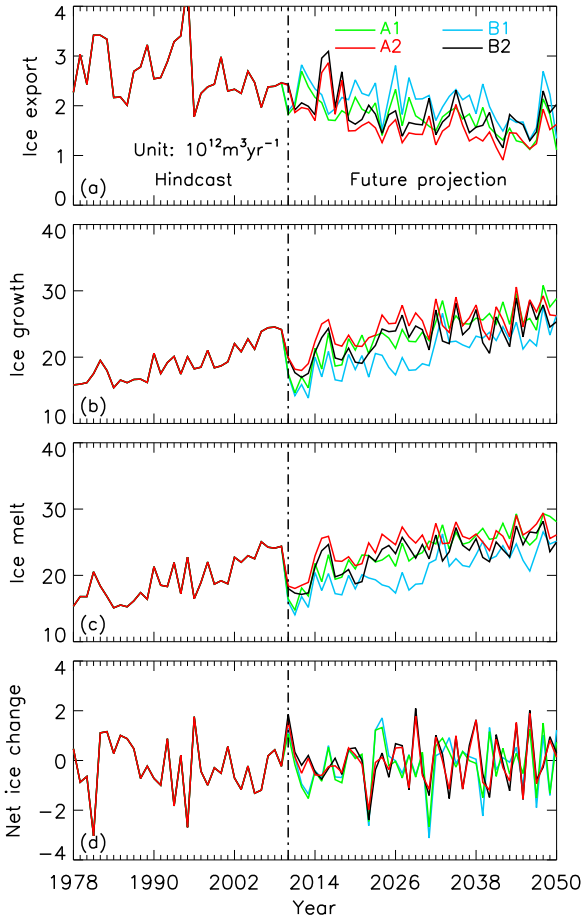

Figure 3. (a) Hindcast and future projections of annual mean ice export, (b) thermodynamic ice growth, (c) ice melt, and (d) net ice change (ice growth minus ice melt and ice export) in the Arctic Ocean.

5. Concluding Remarks

[18] Results from an ice–ocean model indicate that future ice conditions in the Arctic Ocean are sensitive to both AW and CV. Given the substantial CV, it is not likely that the Arctic Ocean will pass a threshold to become ice free in summer permanently before 2050 even though some individual summers may be ice free prior to that year. The absence of a "tipping point" with respect to the loss of summer arctic sea ice in the IPCC GCM simulations [*Winton*, 2006] is also reflected in our simulations.

[19] Because most IPCC GCMs substantially underestimate the summer sea ice extent decline observed in recent years, speculations arise that the Arctic Ocean may become ice free in summer much sooner than most of the GCM projections. Results of this study suggest that for a summer ice-free Arctic Ocean to occur much earlier than 2050,

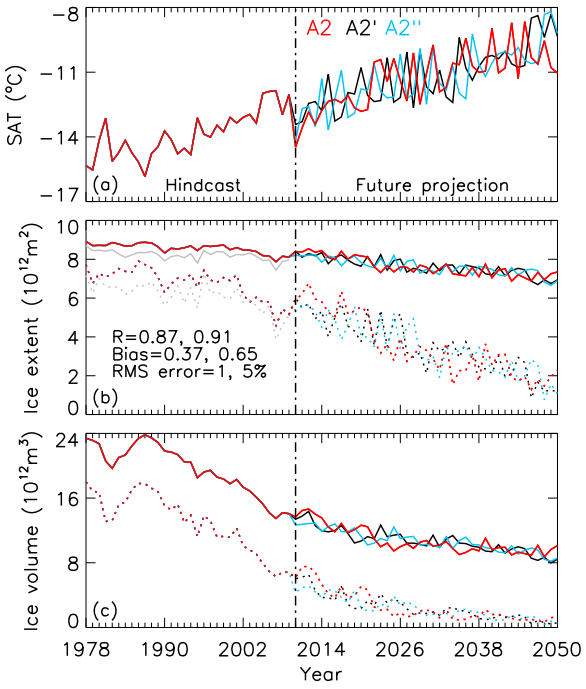

Figure 4. Same as Figures 1b, 1d, and 1c, but for cases A2, A2′, and A2″.

ΔSAT > 4°C is needed. To further support this point, two additional model runs are conducted for the A2 case using two different sets of randomly picked years of forcing from the 1989–2009 pool. The projected sea ice trends and variability from these two runs (denoted as cases A2′ and A2″) do not differ significantly from the A2 results (Figure 4).

[20] **Acknowledgments.** This work was supported by the NSF's Office of Polar Programs and the NASA's Cryosphere Program.

References

Bitz, C. M., and G. H. Roe (2004), A mechanism for the high rate of sea-ice thinning in the Arctic Ocean, *J. Clim.*, *17*, 3622–3632, doi:10.1175/1520-0442(2004)017<3623:AMFTHR>2.0.CO;2.

Hibler, W. D., III, and K. Bryan (1987), A diagnostic ice-ocean model, *J. Phys. Oceanogr.*, *17*, 987–1015, doi:10.1175/1520-0485(1987)017<0987:ADIM>2.0.CO;2.

Holland, M. M., M. C. Serreze, and J. Stroeve (2010), The sea ice mass budget of the Arctic and its future change as simulated by coupled climate models, *Clim. Dyn.*, *34*, 185–200, doi:10.1007/s00382-008-0493-4.

Intergovernmental Panel on Climate Change (IPCC) (2007), *Climate Change 2007: The Physical Science Basis. Contribution of Working Group I to the Fourth Assessment Report of the Intergovernmental Panel on Climate Change*, edited by S. Solomon et al., Cambridge Univ. Press, Cambridge, U. K.

Maslowski, W. (2010), Advancements and limitations in understanding and predicting Arctic climate change, paper presented at the State of the Arctic Conference, Natl. Sci. Found., Miami, Fla. (Available at http://soa.arcus.org/sites/soa.arcus.org/files/sessions/1-1-advances-understanding-arctic-system-components/pdf/1-1-7-maslowski-wieslaw.pdf)

Parkinson, C. L., and W. M. Washington (1979), A large-scale numerical model of sea ice, *J. Geophys. Res.*, *84*, 311–337, doi:10.1029/JC084iC01p00311.

Ridley, J., J. Lowe, C. Brierley, and G. Harris (2007), Uncertainty in the sensitivity of Arctic sea ice to global warming in a perturbed parameter climate model ensemble, *Geophys. Res. Lett.*, *34*, L19704, doi:10.1029/2007GL031209.

Simmonds, I., and K. Keay (2009), Extraordinary September Arctic sea ice reductions and their relationships with storm behavior over 1979–2008, *Geophys. Res. Lett.*, *36*, L19715, doi:10.1029/2009GL039810.

Sou, T., and G. Flato (2009), Sea ice in the Canadian Arctic Archipelago: Modeling the past (1950–2004) and the future (2041–2060), *J. Clim.*, *22*, 2181–2198, doi:10.1175/2008JCLI2335.1.

Stroeve, J., M. M. Holland, W. Meier, T. Scambos, and M. C. Serreze (2007), Arctic sea ice decline: Faster than forecast, *Geophys. Res. Lett.*, *34*, L09501, doi:10.1029/2007GL029703.

Wang, M., and J. E. Overland (2009), A sea ice free summer Arctic within 30 years?, *Geophys. Res. Lett.*, *36*, L07502, doi:10.1029/2009GL037820.

Winton, M. (2006), Does the Arctic sea ice have a tipping point?, *Geophys. Res. Lett.*, *33*, L23504, doi:10.1029/2006GL028017.

Zhang, J., M. Steele, R. W. Lindsay, A. Schweiger, and J. Morison (2008), Ensemble one-year predictions of arctic sea ice for the spring and summer of 2008, *Geophys. Res. Lett.*, *35*, L08502, doi:10.1029/2008GL033244.

A. Schweiger, M. Steele, and J. Zhang, Polar Science Center, Applied Physics Laboratory, University of Washington, 1013 NE 40th St., Seattle, WA 98105, USA. (zhang@apl.washington.edu)